Bioconjugate Chemistry

Article

pubs.acs.org/bc

Covalent Immobilization of Proteins on 3D Poly(acrylic acid) Brushes: Mechanism Study and a More Effective and Controllable Process

Zhenyuan Qu, Kaimin Chen, Hongchen Gu, and Hong Xu*

Shanghai Engineering Research Center of Medical Device and Technology at Med-X, School of Biomedical Engineering, Shanghai Jiao Tong University, 1954 Huashan Road, Shanghai 200030, China

Supporting Information

ABSTRACT: Polymeric brushes have emerged as a novel 3D material platform that provides great amounts of binding sites for biomolecules. This paper investigates the covalent immobilization mechanism of protein by spherical poly(acrylic acid) brushes (SPAABs) in the widely adopted *N*-hydroxysuccinimide/*N*-(3-dimethyl-aminopropyl)-*N*′-ethylcarbodiimide hydrochloride (NHS/EDC) process. It was discovered that electrostatic interaction plays a crucial role in the covalent immobilization of protein. Due to the existence of 3D architecture and "Donnan effect", SPAABs exhibit quite different immobilization kinetics in comparison with conventional 2D materials. Under conditions favorable to electrostatic interaction, the effect of "electrostatic interaction induced covalent binding" was observed as a result of competitive immobilization by physical adsorption and chemical binding. On the basis of the mechanism study, a new "chemical conjugation after electrostatic entrapment" (CCEE) method was developed which set the chemical and physical immobilization process apart. A more effective and well-defined covalent immobilization was achieved. And the binding capacity can be tuned in a wide range (0−4.2 mg protein/mg SPAABs) with a high level of control.

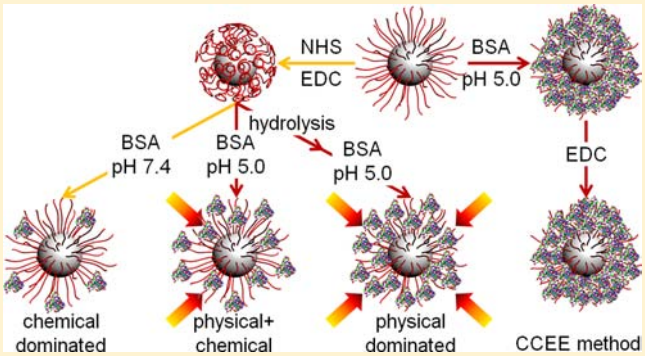

INTRODUCTION

Polymeric brushes have emerged as a promising material platform for a wide range of biomedical applications.[1−8] One of the most prominent features of the brushes lies in their three-dimensional (3D) structure with abundant functional groups that can be used to bind multilayer biomolecules (such as proteins) with a variety of strategies.[9] In particular, poly(acrylic acid) (PAA) brushes have aroused considerable interest due to their properties of high swelling in aqueous solution and rich content of carboxyl groups, which facilitates the immobilization of multilayer proteins with high binding capacity.[4,5,7,10−12]

Physical adsorption is the most straightforward way for protein immobilization, which takes place via electrostatic interactions between anionic PAA chains and the positive "patches" on proteins.[13] The PAA brushes were shown to adsorb large amounts of proteins with both the opposite[11,14] and same charge.[10,15] For the latter unusual case, comprehensive studies by the Ballauff's and Czeslik's groups have elucidated the mechanism of "counterion release" on both spherical[10,16−19] and planar PAA brushes,[14,20,21] as well as other polyelectrolyte brushes,[22−24] when the proteins are adsorbed into polyelectrolyte brushes on the "wrong side" of their isoelectric point (pI). Furthermore, this process was shown to largely preserve the secondary structure of proteins[25] or the activity of enzymes[2,26,27] with spherical PAA brushes (SPAABs), making them a promising carrier for potential biomedical applications. In spite of the high binding capacity and protein activity, physical adsorption is susceptible to the change of media environment (pH, salt concentration, etc.), which prevents their further application in complex biological media.[26]

To overcome the intrinsic instability of physical immobilization, two other strategies have been employed, i.e., covalent binding and metal-ion affinity method. The latter, relying on the coordination interaction between histidine residues on the protein and metal-complex on the material, requires derivation of PAA brushes before protein immobilization.[4,11] Comparatively, covalent immobilization via the well-established *N*-hydroxysuccinimide/*N*-(3-dimethyl-aminopropyl)-*N*′-ethylcarbodiimide hydrochloride (NHS/EDC) process is more widely used, forming robust amide linkage between carboxyl groups on PAA brushes and amino groups on proteins.[9,28] The ubiquity of amino and carboxyl groups in proteins and the common existence of these two functional groups on materials, together with the excellent efficiency and biocompatibility of the reaction, renders the NHS/EDC process a versatile, even irreplaceable method in bioconjugation.[29]

The PAA brushes, with abundant carboxyl groups, are considered particularly suitable for the NHS/EDC process. Although plenty of works have reported the utilization of PAA

Received: November 15, 2013
Revised: December 26, 2013
Published: December 28, 2013

brushes or materials grafted with PAA segments to achieve an enhanced covalent immobilization of proteins,[3−5,11,12,30] few works paid attention to the effectiveness of this process applied to PAA brushes. As a matter of fact, among the few works that reported the quantitative protein binding capacity results,[4,11,12] the performance of PAA brushes as well as the binding capacity vary to a large degree with different proteins. In addition, both ref 11 and ref 4 explicitly reported a lower binding capacity for NHS/EDC process than the metal-ion affinity method, which is even lower than that which can be achieved with physical adsorption.[31] The results indicate that, to achieve covalent immobilization of proteins, the current NHS/EDC process may significantly sacrifice the potential of PAA brushes, and the immobilization mechanism is rather unclear compared with the physical adsorption process.

In this paper, we present the first study on the immobilization mechanism of NHS/EDC process for SPAABs using BSA as model protein. The immobilization kinetics is carefully examined and the unique behavior of SPAABs in this process is shown by comparing with the conventional carboxylated particles. Based on our mechanism study, a new covalent immobilization method is developed. We show that effective and tunable covalent immobilization of proteins can be fulfilled by the new method in a well-defined and highly controlled manner.

EXPERIMENTAL SECTION

Materials. BSA was purchased from Sigma-Aldrich. EDC was obtained from Aladdin Reagent (Shanghai) Co., Ltd. NHS was obtained from Thermo Scientific. All other reagents used in this work were the products of China National Medicines Group Shanghai Chemical Reagents Company.

Ten micromolar phosphate buffer (PB, pH = 7.4, containing 0.05 wt % Tween-20) and 2-(*N*-morpholino)ethanesulfonic acid buffer (MES, pH = 5.0, containing 0.05 wt % Tween-20) were used in the protein binding experiments. Phosphate Buffered Saline (PBS) used for the protein desorption is prepared by adding 150 mM NaCl into PB.

SPAABs with an 85 nm SiO_2 core and conventional carboxylated SiO_2 particles (SiO_2−COOH) with a similar size were used in the study of protein binding mechanism in NHS/EDC conjugation process. The synthesis and characterization of SPAABs was done as described recently.[12] The preparation of SiO_2−COOH was conducted according to the literature.[32] Key structural parameters are listed in Table 1 and defined as follows:

Table 1. Characterization of SPAABs and SiO_2−COOH[a]

particles	D_c (nm)	L (nm)	N (mmol/g)	σ (nm^{-2})
SPAABs	85	39	1.88	0.24
SiO_2−COOH	90	5	0.05	1.0

[a] D_c, diameter of the core; L, thickness of the modification layer; N, content of carboxyl groups; σ, grafting density of PAA chains or carboxyl groups (see Experimental Section for measurement methods).

D_c: Diameter of the SiO_2 core measured from transmission electron microscope (TEM) image. The number-average diameter obtained by dynamic light scattering (DLS) is about 10 nm larger than the TEM diameter.

L: Thickness of the particle's modification layer defined as the increase in hydrodynamic radius (measured by DLS in 10 mM PB, pH = 7.4) after modification.

N: Content of carboxyl groups characterized by conductometric titration for SPAABs. For SiO_2−COOH, the content of carboxyl groups was quantified by a more sensitive colorimetric method reported in ref 33 after the activation by NHS, assuming that the activation reaction is quantitative.[34,35] The same method was employed in the analysis of hydrolysis kinetics of NHS ester for SPAABs.

σ: Grafting density of PAA chains or carboxyl groups on the silica core calculated from N and the molecular weight (M_n) of the modification layer. To calculate the specific surface area, the silica core is regarded as solid spheres with a density of 2 g/cm^3. The M_n of PAA brushes was determined to be 12.6 kDa with a PDI of 1.05 by gel permeation chromatography (Agilent 1260 MDS) equipped with a differential refractometer and light scattering detector.

Protein Immobilization. For NHS/EDC conjugation, the particles were transferred into MES by washing with the buffer two times. The particles were activated for 20 min at ambient temperature with the addition of 0.2 M NHS and EDC. The excessive reactants were removed by centrifugation and washing with MES three times. To guarantee a low and controlled hydrolysis degree of NHS ester, the activation and washing procedure in all experiments were done in an acidic MES buffer with the washing time strictly controlled within 30−40 min. After discarding the supernatant, the particles were dispersed in target buffer (PB, pH 7.4 or MES, pH 5.0) with 1 mg/mL protein and incubated at 25 °C to allow the conjugation. After conjugation, the particle−protein complexes were washed two times with PBS and dispersed in PBS.

For the physical adsorption, the particles were transferred into PB or MES by washing with the target buffer two times. After discarding the supernatant, the protein dissolved in the corresponding buffer (1 mg/mL) was charged and mixed with particles. The mixture was incubated at 25 °C for 2 h to allow the physical adsorption, and desorption was done by washing the particle−protein complexes two times with PBS.

For chemical conjugation after electrostatic entrapment (CCEE) method, the protein was first entrapped into the SPAABs in MES via electrostatic interaction using the above physical adsorption protocol. Then, the particle−protein complexes were washed two times by MES before the conjugation with 5 mM EDC in MES. After conjugation, the particle−protein complexes were redispersed in PBS by washing two times with PBS.

The protein concentration was quantified by BCA protein quantification method. The protein contents in the original protein solution, supernatant in binding, and washing solution in each step were measured to obtain the binding capacity on the particles. For NHS/EDC conjugation process, a control sample without the addition of protein is set to eliminate the interference from NHS hydrolyzed from the activated particles.

RESULTS AND DISCUSSION

Protein Immobilization Mechanism of NHS/EDC Process in SPAABs. *Results.* The SPAABs used in this study are monodispersed colloidal particles with an 85 nm SiO_2 core and densely grafted PAA chains synthesized via surface RAFT polymerization.[12] As a comparison, conventional carboxylated SiO_2 particles (SiO_2−COOH) with a similar core size were synthesized using a reported method.[32] Key

dx.doi.org/10.1021/bc400530s | Bioconjugate Chem. 2014, 25, 370−378

structural parameters of the two particles are listed in Table 1 and a schematic representation of the two particles and the NHS/EDC process is shown in Scheme 1.

Scheme 1. Illustration of the Structure of SPAABs and SiO_2−COOH and the NHS/EDC Covalent Immobilization Process

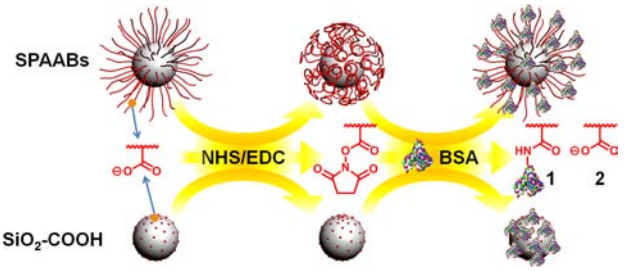

In the NHS/EDC process, carboxyl groups on the materials are first converted to NHS ester intermediate in the presence of EDC (activation) followed by its reaction with amino groups on the protein (conjugation), forming robust amide linkage (Scheme 1, product **1**). Excess EDC is removed by washing before the addition of proteins to avoid self-polymerization of proteins. During washing and conjugation steps, the unreacted NHS ester will undergo hydrolysis and turn back to carboxyl groups (Scheme 1, product **2**), which is the major competing side reaction. The conjugation is usually conducted in a neutral or slightly basic environment to maintain high reactivity of amino groups on the protein, while the activation step is preferentially done in an acidic buffer to improve the stability of NHS ester intermediate.[36] Our preliminary experiment, however, reveals that conjugation of BSA by SPAABs in PB (10 mM, pH = 7.4) results in very ineffective binding with the capacity of 122 μg/mg, close to the maximum of monolayer coverage (C_{max}, about 400 ng/cm^2,[11] corresponding to 136 μg/mg for 85 nm silica particles). This result is similar to that reported by Dai,[11] who attributes it to the hydrolysis of the NHS ester. On the other hand, it has also been mentioned[3] that conjugation done in an acidic MES buffer (pH = 5.0) will afford a higher binding capacity for the acidic BSA (pI ∼ 5, Figure S1 in Supporting Information), which implies the important role of electrostatic interaction in the NHS/EDC process. On the basis of these preliminary results, we conducted a careful investigation on the immobilization mechanism of the NHS/EDC process in PAA brushes.

To begin with, we measured the binding capacities of BSA to SPAABs and SiO_2−COOH in two buffers via NHS/EDC (chemical) process and electrostatic interaction (physical). The results are summarized in Table 2. As expected, the results of physical processes clearly show that the electrostatic interaction between BSA and carboxylated materials is favored in MES (entry 3 vs 1, entry 7 vs 5). For SPAABs, an exceptionally high binding capacity is obtained under favorable conditions (entry 3) due to the entry of proteins into their 3D structure by electrostatic driving force.[37] When it comes to the chemical process, for both particles, higher binding capacities are obtained in MES, a condition that is unfavorable to chemical conjugation. These results, however, are generally in line with the previous reports on a 2D SAMs[35] and a planar PAA brushes system,[3] respectively; and in all cases (except entry 3 and 4), the chemical binding capacities are close to the physical in the same buffer, indicating the influence of electrostatic interaction

Table 2. Binding Capacity of SPAABs and SiO_2−COOH in PB and MES with Different Binding Processes

entry	sample	buffer	process	binding capacity (μg/mg)[a]	desorption (μg/mg)[b]
1	SPAABs	PB	physical	99	12
2	SPAABs	PB	chemical	122	0
3	SPAABs	MES	physical	868	776
4	SPAABs	MES	chemical	335	29
5	SiO_2−COOH	PB	physical	0	0
6	SiO_2−COOH	PB	chemical	25	0
7	SiO_2−COOH	MES	physical	97	56
8	SiO_2−COOH	MES	chemical	83	0

[a]Immobilization was done at 25 °C for 21 h. [b]Desorption was done in PBS, and the protein released into the supernatant was quantified after centrifugation of particles.

on the covalent immobilization process. Among all results, entry 4 is rather eye-catching. On one hand, the binding capacity reaches 2.5-fold of C_{max} (much higher than entry 2), suggesting the entry of protein during the immobilization process. On the other hand, it is significantly lower than entry 3. The desorption experiments carried out in PBS reveal the distinct difference between physical and chemical immobilization. The chemical immobilization is stable while the physical adsorption is, to a large degree, vulnerable to the change of buffer conditions.[38]

To explain the result of entry 4, we examined the hydrolysis and immobilization kinetics of NHS-activated SPAABs in PB and MES. As shown in Figure 1a, hydrolysis in both buffers exhibits the pseudo-first-order kinetics to the concentration of NHS ester ([OH^-] can be regarded as constant).[39] A rapid hydrolysis of NHS ester in PB with a half-life time ($t_{1/2}$) of 37 min is observed, in accordance with that observed by Dai.[11] As expected, a larger $t_{1/2}$ of 2.5 h is obtained in MES, indicating a much higher stability of NHS ester in acidic environment. The BSA immobilization kinetics are shown in Figure 1b. The kinetics of SPAABs in MES is quite different from that in PB. While the latter quickly levels off within 2 h, the former increases continuously to a much higher plateau at about 10 h, and their disparity enlarges with the increase of time. As comparison, kinetics of SiO_2−COOH are akin to that of SPAABs in PB with even lower binding capacities. Two possible explanations may be given to the higher binding capacity and unique immobilization kinetics for SPAABs in MES. (1) Electrostatic interaction dominant hypothesis: the higher binding capacity in MES is due to a favorable electrostatic interaction and the slow increase of binding capacity is because of the hydrolysis of NHS ester, which increases the binding sites via electrostatic interaction with the recovery of carboxyl groups. (2) Chemical reaction dominant hypothesis: the higher binding capacity in MES is due to increased reactive sites rendered by slower hydrolysis of NHS ester, and the slow increase of binding capacity is a result of slow reaction kinetics between BSA and NHS-activated SPAABs in MES.[11]

An experiment was designed to discriminate the above two hypotheses and further elucidate the immobilization mechanism. The NHS-activated SPAABs were dispersed in MES for different time periods to allow a different degree of hydrolysis

dx.doi.org/10.1021/bc400530s | Bioconjugate Chem. 2014, 25, 370−378

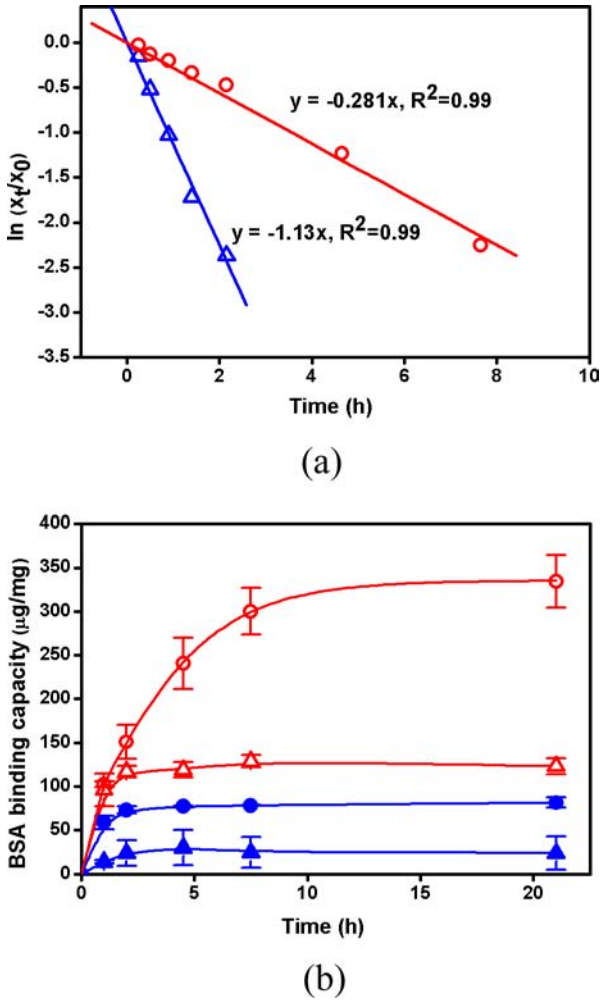

Figure 1. (a) Hydrolysis kinetics of NHS-activated SPAABs in PB (blue △) and MES (red ○). x_t/x_0 means the fraction of residue NHS ester at the time point of t relative to the time point of 0. The data were fitted by linear regression. (b) Conjugation kinetics of BSA to the NHS-activated SPAABs and SiO_2−COOH in PB and MES (red ○) SPAABs in MES (red △) SPAABs in PB (blue ●) SiO_2−COOH in MES (blue ▲) SiO_2−COOH in PB.

before the addition of BSA. The binding capacities of BSA in MES and the corresponding desorption in PBS were plotted as a function of hydrolysis time in Figure 2. For SPAABs, the same trend of increasing protein binding capacity in parallel with an increased hydrolysis degree of NHS ester is observed with an even higher plateau reached at about 10 h. As hydrolysis leads to the decrease of chemical binding sites and the concomitant increase of physical binding site, the results directly substantiate hypothesis 1 and negate hypothesis 2, demonstrating the governing role of electrostatic interaction in covalent immobilization process. It is also worth mentioning that the conjugation time for all points in this experiment was kept as 2 h, showing that the high binding capacity can be obtained within a relatively short time period. Therefore, the slow increase of binding capacity in MES (up to 10 h) in Figure 1b cannot be attributed to the slow reaction kinetics. Furthermore, the desorption experiment explicitly shows the increase of physically adsorbed proteins with the increase of NHS ester hydrolysis degree. At 21 h, the NHS-activated SPAABs turn essentially the same to the unactivated brushes, and at this point the binding capacity becomes close to that obtained by

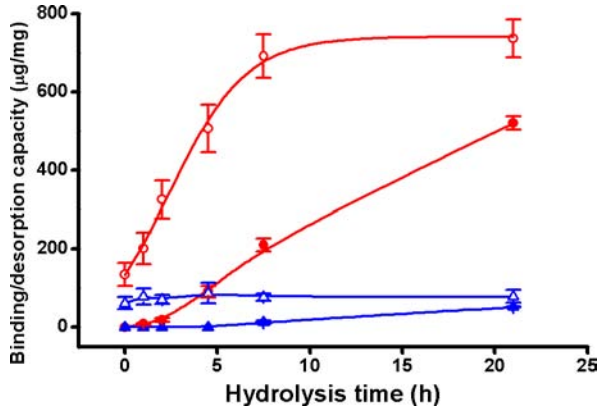

Figure 2. Protein conjugation to partially NHS-activated SPAABs and SiO_2−COOH in MES and desorption with PBS as a function of hydrolysis time. The particles were first activated by NHS in the presence of EDC. After removal of excess EDC and NHS, the NHS-activated particles were dispersed in MES for different time periods before the addition of BSA to obtain particles with different degrees of NHS activation. The conjugation reaction time was kept as 2 h. (red ○) SPAABs binding in MES, (red ●) SPAABs desorption in PBS, (blue △) SiO_2−COOH binding in MES, (blue ▲) SiO_2−COOH desorption in PBS.

physical adsorption. In comparison, the binding capacity of the SiO_2−COOH remains constant regardless of the hydrolysis degree of the NHS ester. The huge differences in binding capacities between SPAABs and SiO_2−COOH in MES (Figure 2 and Figure 1b) are ascribed to the contribution of the inner binding sites of SPAABs with the hydrolysis of NHS ester.

DISCUSSION

The above results reveal that what happened in the NHS/EDC process for SPAABs can be deduced as the integrated process of physical and chemical interaction between SPAABs and proteins (Scheme 2). All findings can be further explained as follows.

Scheme 2. Illustration on the Binding Mechanism of BSA to SPAABs in NHS/EDC Conjugation Processes[a]

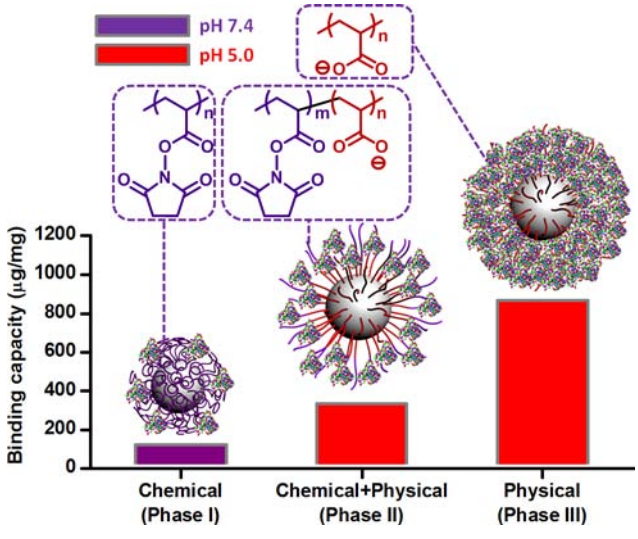

[a]The chemical structures of the monomer unit of SPAABs in different stages are shown in the dashed circles.

dx.doi.org/10.1021/bc400530s | Bioconjugate Chem. 2014, 25, 370−378

1. For physical adsorption (phase III), electrostatic interaction is the dominant driving force leading to the uptake of protein into SPAABs. The whole picture has been clearly depicted by the Ballauff's group.[13] Here, steric hindrance plays a minor role. Although the diameter of BSA (~7 nm) is larger than the distance between two neighboring PAA chains (2.0 nm at the SiO_2 surface and 3.8 nm at the outer layer), the reversible physical adsorption makes it possible for the proteins to rearrange their position in the brushes together with the conformational change of PAA chains, thus rendering the sterically disadvantageous sites available for protein immobilization. As a result, high binding capacity is obtained.

2. For NHS/EDC conjugation done under conventional conditions (phase I), we see a totally different picture. First, the electrostatic driving force is destroyed and suppressed from two aspects: (1) Structure of brushes: NHS activation eliminates the electrostatic binding sites and destroys the structure of SPAABs by converting them into plain uncharged brushes, where the "Donnan effect"[13,40] of PAA brushes vanishes. (2) Binding pH: conjugation in neutral or slightly basic buffer suppresses the electrostatic interaction between PAA brushes and BSA. Second, steric hindrance becomes decisive to chemical reaction. Without the electrostatic driving force, it is difficult for the large BSA molecules to diffuse into the reactive sites that are deeply buried in the dense brushes,[41] and the increasing grafting density of PAA chains close to the core generates an even larger steric hindrance for the deep entry of the protein. Finally, the robust and irreversible covalent binding of BSA molecule cross-links a number of surrounding PAA chains and precludes the possibility of protein rearrangement, which in turn becomes a greater obstacle for the entry of other protein molecules. Consequently, low binding capacity is obtained.

3. Phase II presents the most interesting behavior of SPAABs where the conjugation is done in a physical adsorption favorable buffer. A series of medium binding capacities are obtained as a result of competing immobilization with chemical reaction and electrostatic interaction. With the hydrolysis of NHS ester (either before or during conjugation step), the brushes are essentially the copolymer of acrylic acid and acrylic acid NHS ester. "Electrostatic interaction induced chemical binding" is observed as a part of the proteins entered into the brushes driven by electrostatic interaction and reacted with the unhydrolyzed NHS ester inside SPAABs. In addition, the portion of physical and chemical immobilization changes dynamically with the hydrolysis.

Scheme 3 illustrates the uniqueness of the 3D SPAABs in protein immobilization compared with 2D SiO_2−COOH. For conventional 2D carboxylated materials, hydrolysis does not influence protein binding capacity because the largest protein coverage will not exceed one monolayer (either by physical adsorption or covalent binding). As the "parking area" of a protein is considerably larger than the carboxyl groups, covalent immobilization will be formed with no differences until the majority of NHS esters are hydrolyzed before the addition of proteins (about 7.5 h in Figure 2). On the other hand, the 3D architecture and "Donnan effect" present in SPAABs will absorb protein into their polymer matrix, which, combined with the dynamic hydrolysis process, results in their unique behavior of "electrostatic interaction induced chemical binding".

The above binding mechanism can be used to explain the great disparity in binding capacities obtained by the NHS/EDC process in literature. While both ref 11 and ref 4 conducted the

Scheme 3. Comparison of Protein Immobilization Mechanisms between 3D SPAABs and 2D SiO_2−COOH in NHS/EDC Process

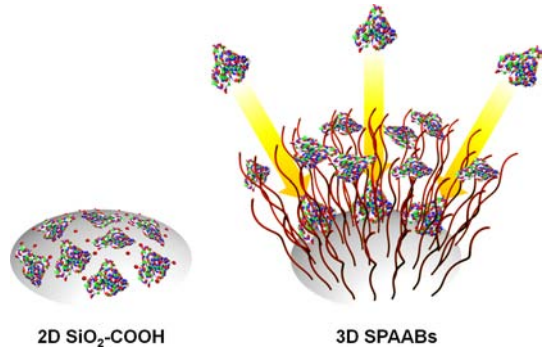

conjugation in a neutral or slightly basic condition, the binding condition of BSA in the former is disadvantageous to physical adsorption, leading to a low binding capacity (phase I in Scheme 2), whereas the immobilization of RNase A (pI = 9.6) in the latter is physically advantageous, rendering a higher binding capacity (corresponding to phase II in Scheme 2). Additionally, the weak dependence of binding capacity on the brush thickness in the former indicates the existence of large steric hindrance, while the linear relationship in the latter implies that proteins enter into the brushes, driven by the electrostatic driving force. The high protein binding capacity obtained in our previous work,[12] then, is also a combined result of electrostatic interaction and covalent binding, which is testified by our further experiments (data not shown).

Effective and Tunable Covalent Protein Immobilization. *Chemical Conjugation after Electrostatic Entrapment (CCEE) Method.* The above study reveals some evident drawbacks of the current NHS/EDC process applied to SPAABs or other 3D materials with similar characteristics: (I) The process is complex where the physical and chemical immobilizations intertwine in the same step together with the hydrolysis side reactions. Consequently, the protein binding capacity is quite sensitive to the hydrolysis degree before the addition of protein and will change dynamically during the immobilization process, leading to a low reproducibility. This problem will be especially prominent when the process is done in a buffer with higher pH, where the hydrolysis kinetics is rather fast. (II) NHS activation is redundant. As a matter of fact, the NHS activation inactivates large numbers of inner sites that are originally accessible for protein binding via electrostatic interaction. The activation even destroyed the structure of SPAABs by introducing side reactions[42] and triggering a certain degree of particle aggregation due to the loss of electrostatic stabilization, making the system ill-defined. (III) The obtained binding capacity is much lower than that achievable by simple physical adsorption, resulting in a remarkable sacrifice in the utilization of SPAABs. To overcome these drawbacks, a new covalent immobilization process, named chemical conjugation after electrostatic entrapment (CCEE) method, is developed.

Figure 3a shows the immobilization procedure. (1) Large quantities of proteins are entrapped into PAA brushes via electrostatic interaction. (2) The brush−protein complexes are washed to remove excess proteins in the system. (3) The brush−protein complexes are treated by EDC to convert electrostatic interaction into covalent binding. (4) The complexes are redispersed in target media for subsequent

dx.doi.org/10.1021/bc400530s | Bioconjugate Chem. 2014, 25, 370−378

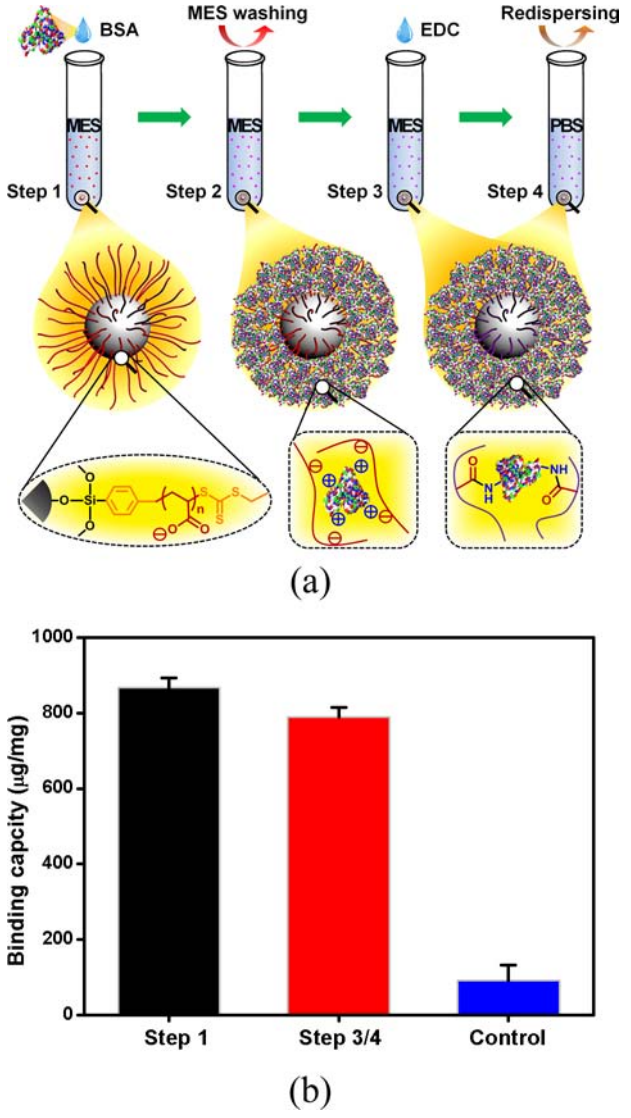

Figure 3. (a) Covalent binding of protein to PAA brushes by CCEE method. (b) Binding capacity of BSA to SPAABs in different Steps. The control underwent the same processes without the addition of EDC.

applications. The corresponding binding capacities are shown in Figure 3b. A high binding capacity (868 μg/mg) is achieved in step 1 and effectively converted to covalent binding by EDC in step 3 with a capacity of 790 μg/mg. With the robust covalent binding, the SPAABs–BSA complex can be redispersed into any target media (such as PBS) without change in protein binding capacity. On the other hand, the control group without treatment by EDC experiences a remarkable release of proteins in the same condition. To further confirm the result, the SPAABs-BSA complexes were subject to thermogravimetric analysis after intensive washing (Figure S2 in Supporting Information). The additional weight loss, corresponding to a binding capacity of 840 μg/mg, is in good agreement with that obtained by the protein quantification method.

The CCEE method takes full advantage of the unique structure and properties of SPAABs. Blessed with their "Donnan effect", large quantities of protein can be immobilized into the 3D architecture without disruption of the brush structure. What is more, the nonequilibrium nature of electrostatic interaction[17] allows the incorporation of washing step (step 2) before EDC conjugation with little loss in binding capacity (as high as 90% of the immobilized proteins were retained). Thus, the CCEE method is composed of tandem physical and chemical immobilization processes that are totally separated from each other. Compared with the conventional NHS/EDC process, the CCEE method is more simple, well-defined, and effective. No activation or derivatization of PAA brushes is needed, and higher binding capacity (close to physical adsorption) can be obtained with better controllability.

Influence of Environmental Conditions. Influence of several environmental parameters including the EDC concentration, pH of binding solution, and temperature was studied. In this method, EDC has dual identities: salt and coupling agents. A low salt concentration needs to be maintained for effective uptake and entrapment of protein. Use of high EDC concentration (~100 mM), while ensuring a quantitative conjugation, will disturb the Donnan equilibrium and give rise to the protein release before the coupling reaction is completed (data not shown). We found that a 5 mM EDC was sufficient to fully convert the proteins from electrostatic interaction into covalent binding without influencing the Donnan equilibrium.

The influence of pH and temperature on the binding capacity is presented in Figure 4. The optimal pH is around 4.5 and the effective binding takes place at pH 3.5–6.1 (Figure 4a). The binding capacity increases slightly with the increase of temperature from 4 to 37 °C (pH = 4.5, Figure 4b) as a result of entropy-driven adsorption,[21] but the effective binding can be conducted at least at any temperature within this range. In all cases, the covalent immobilization capacity is greatly influenced by the electrostatic entrapment in step 1. The wide range of binding conditions provides great flexibility for our method. In the following experiment, we employed the optimal condition, i.e., 37 °C in 10 mM MES (pH = 4.5) with 5 mM EDC for the conjugation.

Influence of SPAABs Structural Parameters. Finally, the influence of SPAAB structural parameters was investigated. The surface RAFT polymerization provides a powerful tool for the synthesis of SPAABs with a high level of control and tunability.[12] Brushes with different grafting densities (0.06, 0.26, and 0.54 chain/nm^2 for SPAABs with low, medium, and high densities, respectively) were obtained from SiO_2 particles with different grafting densities of RAFT chain transfer agent (CTA) while maintaining the feed ratio of monomer to RAFT CTA constant (Figure S3 in Supporting Information); and brushes with different thicknesses (L = 18–145 nm) were prepared from the same RAFT CTA modified SiO_2 by changing the feed ratio of monomer to RAFT CTA (Figure S4 in Supporting Information).

The influence of grafting density is shown in Figure 5a. A higher binding capacity can be obtained with more densely grafted SPAABs due to a stronger electrostatic interaction rendered by higher charge density.[31] Brushes with medium and high grafting density behave similarly in entrapping the protein during washing step, with ~90% of the adsorbed protein transformed into covalently bound protein in subsequent conjugation process. On the other hand, the low density brushes, with a grafting density close to the semidilute brushes regime,[41] are more vulnerable to protein leaching, with about 30% of the protein lost during the washing step. Therefore, brushes with high grafting density are more advantageous for improving the adsorption binding capacity and retaining the protein against washing.

dx.doi.org/10.1021/bc400530s | *Bioconjugate Chem.* 2014, 25, 370–378

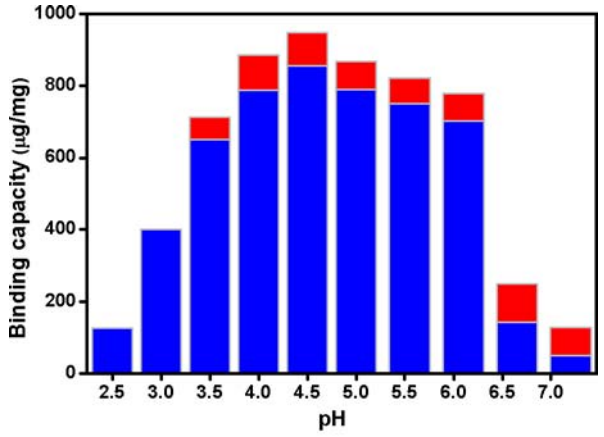

(a)

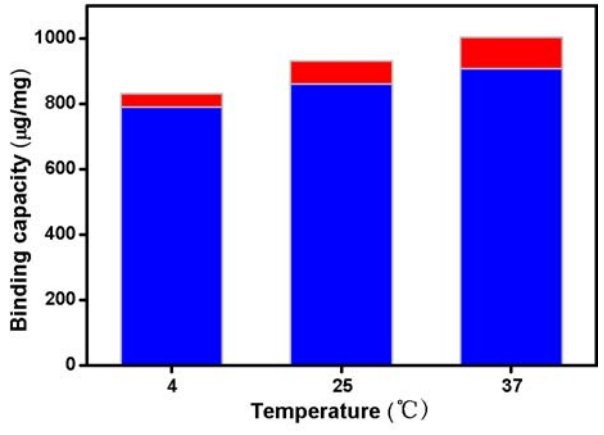

(b)

Figure 4. (a) Influence of pH on the covalent binding capacity at 25 °C. The pH was tuned by adding 0.1 M HCl or NaOH to the 10 mM MES. Aggregation of SPAABs was observed at pH = 2.5. (b) Influence of temperature on the binding capacity. The pH was kept as 4.5 in 10 mM MES. (red ■) excess or weakly adsorbed protein that is washed off by MES. (blue ■) covalently bonded proteins. The results are presented as the average of three independent experiments (2% error).

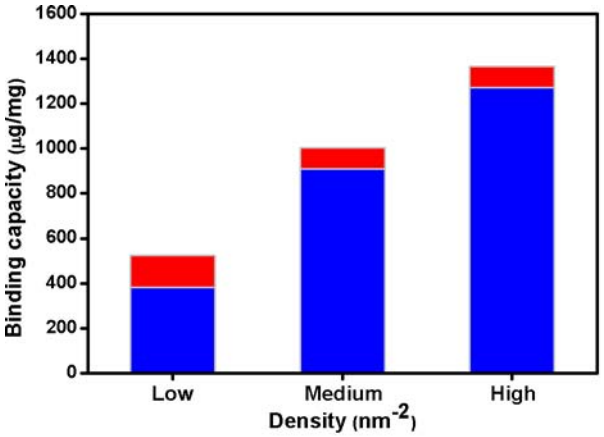

(a)

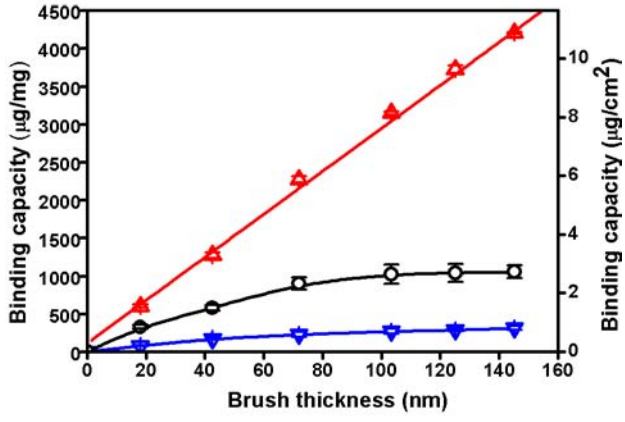

(b)

Figure 5. (a) Influence of grafting density of PAA brushes on the protein binding capacity. The grafting densities are 0.06, 0.26, and 0.54 chain/nm^2 for SPAABs with low, medium, and high densities, respectively. (red ■) excess or weakly adsorbed protein that is washed off by MES. (blue ■) covalently bonded proteins. (b) Influence of brush thickness on the protein binding capacity in different binding processes. (red △) covalent binding by CCEE method (○) covalent binding by NHS/EDC method in MES (pH = 5.0) (blue ▽) covalent binding by NHS/EDC method in PB. Data of (red △) are fitted by linear regression while the lines connecting (○) and (blue ▽) are only to guide the eyes. The results are presented as the average of three independent experiments.

The binding capacity of SPAABs as a function of brush thickness is shown in Figure 5b and compared with the NHS/EDC method conducted in PB and MES. Good linearity (R^2 = 0.997) with high binding capacity is observed for CCEE method, which fully embodies the characteristics of 3D materials that the proteins are piled up layer by layer on the third dimension vertical to the particle surface. For NHS/EDC method done in MES and PB, the binding capacities of both processes are significantly lower, and both binding capacities increase with the brush thicknesses initially and then gradually reach a plateau, suggesting the existence of steric hindrance in these processes. It is also worth mentioning that the coefficient of variation (CV) of the CCEE method for each point is lower than 2%. On the other hand, the NHS/EDC process done in MES possesses a much higher CV of 7−12% even if the time of the washing step is strictly controlled. It indicates that the CCEE method has a much better reproducibility due to its well-defined process.

Since the protein binding capacity on 3D brushes is dependent on both the specific surface area and brush thickness, it is tempting to introduce a new parameter τ_v defined as the binding capacity per unit volume (μg/cm^3) to evaluate their spatial utilization. Given the good linearity, τ_v is independent of the brush thickness for the CCEE method and can be obtained from the slope of the fitted line in Figure 5b (when the result is converted into binding capacity per unit area, right y axis) as 0.75 mg/cm^3. For NHS/EDC processes, the τ_v is much smaller and decreases with the increase of brush thickness (although the binding capacity increases monotonously). The τ_v of CCEE method is also about 2−3-fold larger than the metal-ion affinity method reported in refs 4 and 11. Therefore, the CCEE method possesses the highest utilization of the brushes among the currently available chemical immobilization methods.

For biomedical applications, high immobilization capacity of proteins is often pursued to obtain a higher detection

dx.doi.org/10.1021/bc400530s | Bioconjugate Chem. 2014, 25, 370−378

sensitivity[8] or catalysis efficiency.[43] The CCEE method offers the high immobilization capacity as well as wide tunability (0–4.2 mg/mg) with flexible means through changing pH, ionic strength, temperature, brush thickness, and grafting density. Since the structure of the brushes and the binding process of the CCEE method are both well-defined and highly controllable, it presents an excellent model system to study the relationship between protein immobilization capacity and the performance of the carrier in the application. Above all, the robust covalent immobilization makes it possible for the brush–protein complex to transfer into any media dictated by the downstream applications. One basic concern is whether EDC conjugation in the present method will also activate the carboxyl groups on the protein. Further investigation regarding its influence on protein structure and activity is in progress.

CONCLUSION

We have presented a detailed investigation on protein binding mechanism to SPAABs in the widely adopted NHS/EDC process. The whole process can be described as the competitive interaction between chemical binding and physical adsorption of the protein with the hydrolysis of NHS esters. The results of the competitive interaction generate the effect of "electrostatic interaction induced chemical binding" as a unique phenomenon for SPAABs.

A new CCEE method for the covalent protein immobilization on SPAABs has been developed on the basis of mechanism study. Taking advantage of the unique electrostatic driving force and setting the physical and chemical process apart makes the method highly effective, simple, well-defined, and controllable. The method maximizes the potential of SPAABs and offers a wide range of tunability to protein binding capacity (0–4.2 mg/mg) with a variety of means.

The general principles unraveled in the mechanism study may be generally referred by 3D material platforms involved in the NHS/EDC process, and the method developed in this paper can be extended as a versatile method to other polyelectrolyte brushes with conjugatable groups. Exploration on possible biomedical applications based on the present work is underway.

ASSOCIATED CONTENT

Supporting Information

Zeta potential of SPAABs and BSA, thermogravimetric analysis of SPAABs-BSA complex, DLS and thermogravimetric analysis of SPAABs. This material is available free of charge via the Internet at http://pubs.acs.org.

AUTHOR INFORMATION

Corresponding Author

*E-mail: xuhong@sjtu.edu.cn, Phone: +86-21-62933743, Fax: +86-21-62932907.

Notes

The authors declare no competing financial interest.

ACKNOWLEDGMENTS

This work is supported by NSF of China (21075082), 863 High Tech Program (2012AA020103), SJTU funding (YG2012ZD03), SJTU-UM collaborative research projects (12X120010007), and China postdoctoral foundation (12Z102060005).

REFERENCES

(1) Vaisocherová, H., Yang, W., Zhang, Z., Cao, Z., Cheng, G., Piliarik, M., Homola, J. i., and Jiang, S. (2008) Ultralow fouling and functionalizable surface chemistry based on a zwitterionic polymer enabling sensitive and specific protein detection in undiluted blood plasma. *Anal. Chem. 80*, 7894–7901.

(2) Neumann, T., Haupt, B., and Ballauff, M. (2004) High activity of enzymes immobilized in colloidal nanoreactors. *Macromol. Biosci. 4*, 13–16.

(3) Dong, R., Krishnan, S., Baird, B. A., Lindau, M., and Ober, C. K. (2007) Patterned biofunctional poly(acrylic acid) brushes on silicon surfaces. *Biomacromolecules 8*, 3082–3092.

(4) Cullen, S. P., Liu, X., Mandel, I. C., Himpsel, F. J., and Gopalan, P. (2008) Polymeric brushes as functional templates for immobilizing ribonuclease A: study of binding kinetics and activity. *Langmuir 24*, 913–920.

(5) Wang, Y.-M., Cui, Y., Cheng, Z.-Q., Song, L.-S., Wang, Z.-Y., Han, B.-H., and Zhu, J.-S. (2013) Poly(acrylic acid) brushes pattern as a 3D functional biosensor surface for microchips. *Appl. Surf. Sci. 266*, 313–318.

(6) Cullen, S. P., Mandel, I. C., and Gopalan, P. (2008) Surface-anchored poly(2-vinyl-4,4-dimethyl azlactone) brushes as templates for enzyme immobilization. *Langmuir 24*, 13701–13709.

(7) Rutnakornpituk, M., Puangsin, N., Theamdee, P., Rutnakornpituk, B., and Wichai, U. (2011) Poly(acrylic acid)-grafted magnetic nanoparticle for conjugation with folic acid. *Polymer 52*, 987–995.

(8) Huang, C.-J., Li, Y., and Jiang, S. (2012) Zwitterionic polymer-based platform with two-layer architecture for ultra low fouling and high protein loading. *Anal. Chem. 84*, 3440–3445.

(9) Jiang, H., and Xu, F.-J. (2013) Biomolecule-functionalized polymer brushes. *Chem. Soc. Rev. 42*, 3394–3426.

(10) Wittemann, A., Haupt, B., and Ballauff, M. (2003) Adsorption of proteins on spherical polyelectrolyte brushes in aqueous solution. *Phys. Chem. Chem. Phys. 5*, 1671–1677.

(11) Dai, J., Bao, Z., Sun, L., Hong, S. U., Baker, G. L., and Bruening, M. L. (2006) High-capacity binding of proteins by poly(acrylic acid) brushes and their derivatives. *Langmuir 22*, 4274–4281.

(12) Qu, Z., Hu, F., Chen, K., Duan, Z., Gu, H., and Xu, H. (2013) A facile route to the synthesis of spherical poly(acrylic acid) brushes via RAFT polymerization for high-capacity protein immobilization. *J. Colloid Interface Sci. 398*, 82–87.

(13) Welsch, N., Lu, Y., Dzubiella, J., and Ballauff, M. (2013) Adsorption of proteins to functional polymeric nanoparticles. *Polymer 54*, 2835–2849.

(14) Hollmann, O., and Czeslik, C. (2006) Characterization of a planar poly(acrylic acid) brush as a materials coating for controlled protein immobilization. *Langmuir 22*, 3300–3305.

(15) Czeslik, C., Jackler, G., Steitz, R., and von Grünberg, H.-H. (2004) Protein binding to like-charged polyelectrolyte brushes by counterion evaporation. *J. Phys. Chem. B 108*, 13395–13402.

(16) Rosenfeldt, S., Wittemann, A., Ballauff, M., Breininger, E., Bolze, J., and Dingenouts, N. (2004) Interaction of proteins with spherical polyelectrolyte brushes in solution as studied by small-angle x-ray scattering. *Phys. Rev. E 70*, 061403.

(17) Henzler, K., Rosenfeldt, S., Wittemann, A., Harnau, L., Finet, S., Narayanan, T., and Ballauff, M. (2008) Directed motion of proteins along tethered polyelectrolytes. *Phys. Rev. Lett. 100*, 158301.

(18) Czeslik, C., Jackler, G., Hazlett, T., Gratton, E., Steitz, R., Wittemann, A., and Ballauff, M. (2004) Salt-induced protein resistance of polyelectrolyte brushes studied using fluorescence correlation spectroscopy and neutron reflectometry. *Phys. Chem. Chem. Phys. 6*, 5557–5563.

(19) Czeslik, C., Jansen, R., Ballauff, M., Wittemann, A., Royer, C. A., Gratton, E., and Hazlett, T. (2004) Mechanism of protein binding to spherical polyelectrolyte brushes studied in situ using two-photon excitation fluorescence fluctuation spectroscopy. *Phys. Rev. E 69*, 021401.

(20) Czeslik, C., Jackler, G., Steitz, R., and von Gruenberg, H.-H. (2004) Protein binding to like-charged polyelectrolyte brushes by counterion evaporation. *J. Phys. Chem. B 108*, 13395−13402.
(21) Hollmann, O., Gutberlet, T., and Czeslik, C. (2006) Structure and protein binding capacity of a planar PAA brush. *Langmuir 23*, 1347−1353.
(22) Becker, A. L., Welsch, N., Schneider, C., and Ballauff, M. (2011) Adsorption of RNase A on cationic polyelectrolyte brushes: a study by isothermal titration calorimetry. *Biomacromolecules 12*, 3936−3944.
(23) Henzler, K., Haupt, B., Rosenfeldt, S., Harnau, L., Narayanan, T., and Ballauff, M. (2011) Interaction strength between proteins and polyelectrolyte brushes: a small angle X-ray scattering study. *Phys. Chem. Chem. Phys. 13*, 17599−17605.
(24) Henzler, K., Haupt, B., Lauterbach, K., Wittemann, A., Borisov, O., and Ballauff, M. (2010) Adsorption of β-lactoglobulin on spherical polyelectrolyte brushes: direct proof of counterion release by isothermal titration calorimetry. *J. Am. Chem. Soc. 132*, 3159−3163.
(25) Wittemann, A., and Ballauff, M. (2004) Secondary structure analysis of proteins embedded in spherical polyelectrolyte brushes by FT-IR spectroscopy. *Anal. Chem. 76*, 2813−2819.
(26) Haupt, B., Neumann, T., Wittemann, A., and Ballauff, M. (2005) Activity of enzymes immobilized in colloidal spherical polyelectrolyte brushes. *Biomacromolecules 6*, 948−955.
(27) Henzler, K., Haupt, B., and Ballauff, M. (2008) Enzymatic activity of immobilized enzyme determined by isothermal titration calorimetry. *Anal. Biochem. 378*, 184−189.
(28) Rusmini, F., Zhong, Z., and Feijen, J. (2007) Protein immobilization strategies for protein biochips. *Biomacromolecules 8*, 1775−1789.
(29) Hermanson, G. T. (2008) *Bioconjugation Techniques*, 2nd ed., pp 219−233, Chapter 3, Academic Press, San Diego.
(30) Audouin, F., Larragy, R., Fox, M., O'Connor, B., and Heise, A. (2012) Protein immobilization onto poly(acrylic acid) functional macroporous PolyHIPE obtained by surface-initiated ARGET ATRP. *Biomacromolecules 13*, 3787−3794.
(31) de Vos, W. M., Biesheuvel, P. M., de Keizer, A., Kleijn, J. M., and Cohen Stuart, M. A. (2008) Adsorption of the protein bovine serum albumin in a planar poly(acrylic acid) brush layer as measured by optical reflectometry. *Langmuir 24*, 6575−6584.
(32) Yanqing, A. (2007) Preparation and self-assembly of carboxylic acid-functionalized silica. *J. Colloid Interface Sci. 311*, 507−513.
(33) Tyllianakis, P. E., Kakabakos, S. E., Evangelatos, G. P., and Ithakissios, D. S. (1994) Direct colorimetric determination of solid-supported functional groups and ligands using bicinchoninic acid. *Anal. Biochem. 219*, 335−340.
(34) Sam, S., Touahir, L., Salvador Andresa, J., Allongue, P., Chazalviel, J. N., Gouget-Laemmel, A. C., Henry de Villeneuve, C., Moraillon, A., Ozanam, F., Gabouze, N., and Djebbar, S. (2010) Semiquantitative study of the EDC/NHS activation of acid terminal groups at modified porous silicon surfaces. *Langmuir 26*, 809−814.
(35) Lahiri, J., Isaacs, L., Tien, J., and Whitesides, G. M. (1999) A strategy for the generation of surfaces presenting ligands for studies of binding based on an active ester as a common reactive intermediate: a surface plasmon resonance study. *Anal. Chem. 71*, 777−790.
(36) Hermanson, G. T. (2008) *Bioconjugation techniques*, 2nd ed., pp 171−172, Chapter 2, Academic Press, San Diego.
(37) Ballauff, M. (2007) Spherical polyelectrolyte brushes. *Prog. Polym. Sci. 32*, 1135−1151.
(38) Wittemann, A., Haupt, B., and Ballauff, M. (2007) Controlled release of proteins bound to spherical polyelectrolyte brushes. *Z. Phys. Chem. 221*, 113−126.
(39) Lockett, M. R., Phillips, M. F., Jarecki, J. L., Peelen, D., and Smith, L. M. (2007) A tetrafluorophenyl activated ester self-assembled monolayer for the immobilization of amine-modified oligonucleotides. *Langmuir 24*, 69−75.
(40) de Robillard, Q., Guo, X., Ballauff, M., and Narayanan, T. (2000) Spatial correlation of spherical polyelectrolyte brushes in salt-free solution as observed by small-angle X-ray scattering. *Macromolecules 33*, 9109−9114.
(41) Tsujii, Y., Ohno, K., Yamamoto, S., Goto, A., and Fukuda, T. (2006) Structure and Properties of High-Density Polymer Brushes Prepared by Surface-Initiated Living Radical Polymerization. In *Surface-Initiated Polymerization I* (Jordan, R., Ed.) pp 1−45, Chapter 63, Springer, Berlin Heidelberg.
(42) Wang, C., Yan, Q., Liu, H.-B., Zhou, X.-H., and Xiao, S.-J. (2011) Different EDC/NHS activation mechanisms between PAA and PMAA brushes and the following amidation reactions. *Langmuir 27*, 12058−12068.
(43) Christian Reichhart, C. C. (2010) A quantitative study of the enzymatic activity of horseradish peroxidase at a planar poly(acrylic acid) brush. *Colloids Surf., B 75*, 612−616.